Camptothecin-binding site in human serum albumin and protein transformations induced by drug binding

Fabrice Fleury[a], Anatoli Ianoul[a,c], Maurice Berjot[b], Alexei Feofanov[c], Alain J.P. Alix[b], Igor Nabiev[a,*]

[a] *Laboratoire de Spectroscopie Biomoléculaire, UFR de Pharmacie, Université de Reims Champagne-Ardenne, 51096 Reims Cedex, France*
[b] *Laboratoire de Spectroscopies et Structures Biomoléculaires, UFR Sciences, Université de Reims Champagne-Ardenne/INSERM Unité 314, 51687 Reims Cedex, France*
[c] *Optical Spectroscopy Division, Shemyakin and Ovchinnikov Institute of Bioorganic Chemistry, Russian Academy of Sciences, 117871 Moscow, Russia*

Received 15 May 1997

Abstract Circular dichroism (CD) and Raman spectroscopy were employed in order to locate a camptothecin (CPT)-binding site within human serum albumin (HSA) and to identify protein structural transformations induced by CPT binding. A competitive binding of CPT and 3′-azido-3′-deoxythymidine (a ligand occupying IIIA structural sub-domain of the protein) to HSA does not show any competition and demonstrates that the ligands are located in the different binding sites, whereas a HSA-bound CPT may be replaced by warfarin, occupying IIA structural sub-domain of the protein. Raman and CD spectra of HSA and HSA/CPT complexes show that the CPT-binding does not induce changes of the global protein secondary structure. On the other hand, Raman spectra reveal pronounced CPT-induced local structural modifications of the HSA molecule, involving changes in configuration of the two disulfide bonds and transfer of a single Trp-residue to hydrophilic environment. These data suggest that CPT is bound in the region of inter-domain connections within the IIA structural domain of HSA and it induces relative movement of the protein structural domains.

Key words: Raman spectroscopy; Circular dichroism; Topoisomerase inhibitor; Camptothecin; Human serum albumin

1. Introduction

20(S)-Camptothecin (CPT) and its derivatives, potent antitumour drugs against a wide range of human tumours, exhibit their cytotoxicity by stabilising topoisomerase (topo) I–drug–DNA ternary complexes [1,2]. CPT contains a α-hydroxy δ-lactone ring which was found to be a principal structural requirement for the drug biological action [3]. In whole blood versus plasma, CPT displays enhanced stability due to drug association with the lipid bilayers of red blood cells [4]. Human serum albumin (HSA), a vast mediator of transport and metabolism of numerous pharmaceuticals in the blood, preferentially binds the hydrolysed (carboxylate) form of the drug with a ca. 150-fold higher affinity than the lactone (native) form [5]. These interactions result in CPT opening more rapidly and completely in the presence of HSA. Comparison of drug stability in both plasma and purified serum albumin samples revealed that lactone ring opening occurred to a much greater extent in human samples as related to other species [6]. Moreover, serum albumins from non-human species were found to bind CPT much weaker than HSA. Hence, the question of interactions of CPT with blood components and, particularly with HSA, seems to be extremely important if the problem of drug delivery to its target is concerned.

The structural basis of CPT interactions with HSA remains to be defined. It was noted [4] that crystallographic analysis of CPT/HSA complexes is in progress, but these data have not yet appeared in the literature. Fluorescence spectroscopy studies of Burke et al. [5–7] demonstrated that carboxylate CPT binds to a hydrophobic binding pocket on HSA. Aside from hydrophobic binding, ionic interactions between carboxylate CPT and the protein [7] were also revealed in these studies.

In recent CD and fluorescence investigations of our group [8–10] pronounced differences of interactions of lactone, carboxylate, and self-aggregated forms of CPT with HSA and BSA were found. It was shown that HSA binding changes geometry of CPT's covalent structure resulting from hydrophobic contacts of rings A and B of the chromophore with the protein interior and interactions of carbonyl group of CPT's ring D with the positively charged amino acid residue of HSA. Neither heat-denatured HSA nor native BSA exerted binding of CPT. Analysis of HSA and BSA sequence homology within the IIA and IIIA principal ligand-binding domains led us to prediction that the binding site for the CPT chromophore is located in the subdomain IIA of the HSA structure [10].

In the present report, we employ CD and Raman spectroscopy in order to (i) locate the CPT-binding site within HSA, and (ii) to identify and quantitate conformational changes of the protein induced by CPT binding. The first question is addressed by CD analysis of competitive (with other ligands occupying IIIA or IIA principal ligand-binding HSA structural domains) binding of CPT with HSA. The second problem is resolved by Raman and CD analysis of CPT-induced changes of protein conformation. CPT-binding site is proved to be located within the IIA ligand-binding domain of HSA. Interaction with CPT does not induce significant (within ca. 30 peptide bonds) changes in HSA secondary structure, but altered configuration of at least two disulfide bridges and transfers a single Trp^{214} of HSA (located within the IIA subdomain) from more hydrophobic (in free HSA) to hydrophilic (in HSA/CPT complex) environment. The data suggest that CPT binding induces relative movement of the protein structural domains. This model seems to be in

*Corresponding author. Fax: (33) 3-2682-6001.
E-mail: igor.nabiev@univ-reims.fr

Abbreviations: 20(S)-CPT or CPT, 20(S)-camptothecin; HSA, human serum albumin; BSA, bovine serum albumin; CD, circular dichroism; AZT, azido-3′-deoxythymidine; DMSO, dimethylsulfoxide; PBS, potassium-buffered saline; Topo I, DNA topoisomerase I

PII S0014-5793(97)00693-5

good correlation with homologous multi-domain organisation of the three-dimensional structure of HSA proposed from the X-ray structural analysis of the free native protein [11].

2. Materials and methods

2.1. Chemicals

20(S)-CPT, HSA (fatty acid free), AZT and warfarin were purchased from Sigma and used without further purification. Drug stock solution of CPT was prepared in DMSO (ACS spectrophotometric grade, Aldrich) at a concentration 2×10^{-3} M and stored in the dark at −70°C. By mixing 1 part of drug stock solution in DMSO with 1 part of PBS buffer (pH 10), 1 mM working stock solution of the carboxylate form of the drug was prepared. 2 mM solution of CPT in DMSO was used as a stock of a lactone form. Stock solution of HSA was prepared in PBS buffer (pH 7.5) at a concentration 20 mg/ml. AZT and warfarin were prepared at 100 mM concentrations in PBS (pH 7.5).

For CD measurements, complex of CPT with HSA was prepared by mixing of the component's stock solutions in PBS (pH 7.5) to obtain the final concentrations 4×10^{-5} M of CPT and 3 mg/ml (ca. 4.5×10^{-5} M) of HSA. For Raman spectroscopy, the HSA 20 mg/ml stock solution and HSA/CPT complexes at the final concentrations of 18 mg/ml (HSA) and 2×10^{-4} M (CPT) were used. Only the complexes of HSA with the carboxylate form of CPT were studied by Raman spectroscopy due to the extremely low solubility of the CPT lactone form in the aqueous buffers. The final preparations of complexes studied by both CD and Raman techniques contained 2% DMSO.

2.2. Circular dichroism and Raman spectroscopy

CD spectra were measured with a Jobin Yvon, Mark III dichrograph. Usually CD spectra were recorded using 0.1 mm or 1 cm quartz cells, in a range 420–185 nm with a 1 or 2 s time constant. Protein and CPT concentrations were estimated from their molar absorption coefficients in PBS: $\varepsilon_M{}^{278} = 39\,800$ M^{-1} cm^{-1} and $\varepsilon_M{}^{370} = 19\,900$ M^{-1} cm^{-1}, respectively. UV-vis spectra were recorded with a Philips PU8720 UV/vis scanning spectrophotometer. The CD spectra were scaled to molecular elipticity ($\Delta\varepsilon$).

Raman spectra were recorded with a PHO(CODERG) spectrometer in the frequency range from 300 to 1800 cm^{-1}. 514.5 nm line of the Ar-ion Coherent Radiation (model Innova) laser operating with 400 mW power at the sample, was used for excitation. Data accumulation of 350 independent scans with time averaging was used. The stability of the protein in the process of laser irradiation was controlled by analysis of Raman spectra of HSA as a function of time and by comparison of CD spectra of HSA before and after recording of the Raman spectra.

The treated Raman spectra of HSA and HSA/CPT complexes were obtained as follows. First, we recorded the spectra of HSA (in a PBS solution) and of HSA/CPT complex (in a PBS solution). Then the spectra of PBS and of the mixture of PBS/DMSO/CPT were recorded. After subtracting subsequently PBS spectrum from the spectrum of HSA and PBS/DMSO/CPT spectrum from the spectrum of HSA/CPT complexes, the spectra of HSA and HSA/CPT presented in the paper were obtained.

Spectral decomposition in the regions of disulfide bridges (480–560 cm^{-1}) and environment-sensitive Trp vibrations (1300–1400 cm^{-1}) was performed as described [12]. The quality of decomposition was checked by comparison of the spectra reconstructed from the deconvoluted bands with the experimental spectra. An excellent correlation (with the error $<2\%$) was found between theoretical (reconstructed) and experimental spectra. The procedures were performed using the CurveFit module of the LabCalc package (Galactic Industries). The secondary structures of the protein was calculated using RIP (Reference Intensity Profile) method [12].

2.3. Procedure of competitive binding

Competitive binding CD experiments were employed in order to locate a CPT-binding site of HSA. Titration of the aqueous buffer solution of a HSA/CPT complex by AZT or warfarin was used in attempt to replace a HSA-bound CPT by ligands occupying the binding sites in IIIA (AZT) or IIA (warfarin) domains of the protein. The final molar ratios of the components in AZT/HSA/CPT and warfarin/HSA/CPT mixtures were 1000/1/1, i.e. final concentrations of the components in reaction mixtures were 2000×10^{-5} M (warfarin or AZT), ca. 2×10^{-5} M (HSA), and ca. 2×10^{-5} M (CPT).

3. Results and discussion

3.1. Location of the CPT-binding site of HSA

The topology of HSA is created by a repeating series of six helical subdomains [11]. Consistent with the internal amino-acid sequence homology, there are three structurally homologous domains that repeat in the molecule (denoted I, II, and III). Each domain is formed by two smaller subdomains A and B, as previously described at high resolution X-ray structure of HSA (Fig. 1). Altogether, roughly 67% of HSA is helical, with a remainder in turns and extended polypeptide [11]. Subdomains A and B possess two identical structural motives that includes h1–h4 helices for subdomain A and h7–h10 helices for subdomain B (Fig. 1). In addition to these motives, subdomain A is supplemented by two additional short antiparallel helices, h5 and h6, which are tied together by a pair of disulfide bridges forming a small disulfide double loop. As it was shown from heavy-atom derivative screen and from preliminary binding studies, the main binding regions on HSA are located in subdomains IIA and IIIA [11]. The binding cavity of IIIA is most active and accommodating on HSA. Many ligands were found to bind there (AZT, digitoxin, ibuprofen, tryptophan, etc.). Warfarin occupies a single site in IIA. These observations were based on competitive inhibition and spectroscopic studies [13–15].

We have recently shown that the interaction of camptothecin with HSA induces pronounced optical activity of the drug, whereas neither heat-denatured HSA nor native BSA participated in binding of CPT [8–10]. Analysis of HSA and BSA sequence homology within the principal ligand-binding domains led us to prediction that the binding site for the CPT chromophore is located in subdomain IIA. In order to check this prediction, this paper presents comparative spectroscopic studies of competitive inhibition of the binding of CPT.

Among the other ligands, AZT is a typical and specific IIIA-binder, and warfarin-IIA-binder. The binding constants were found to be ca. 2.5×10^{5} M^{-1} [15]. Neither AZT, nor warfarin exhibit induced optical activity when in complex with HSA, whereas CPT/HSA interactions dramatically increase inherent optical activity of CPT. Hence, competitive binding of CPT with either AZT or warfarin with HSA may be fruitfully studied by means of CD spectroscopy in order to locate the CPT-binding site of the protein.

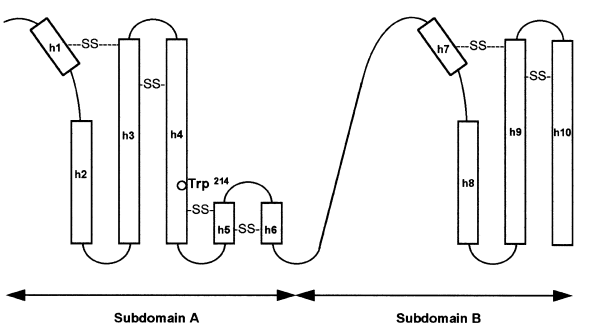

Fig. 1. Schematic presentation of the HSA structural subdomains adapted from [11].

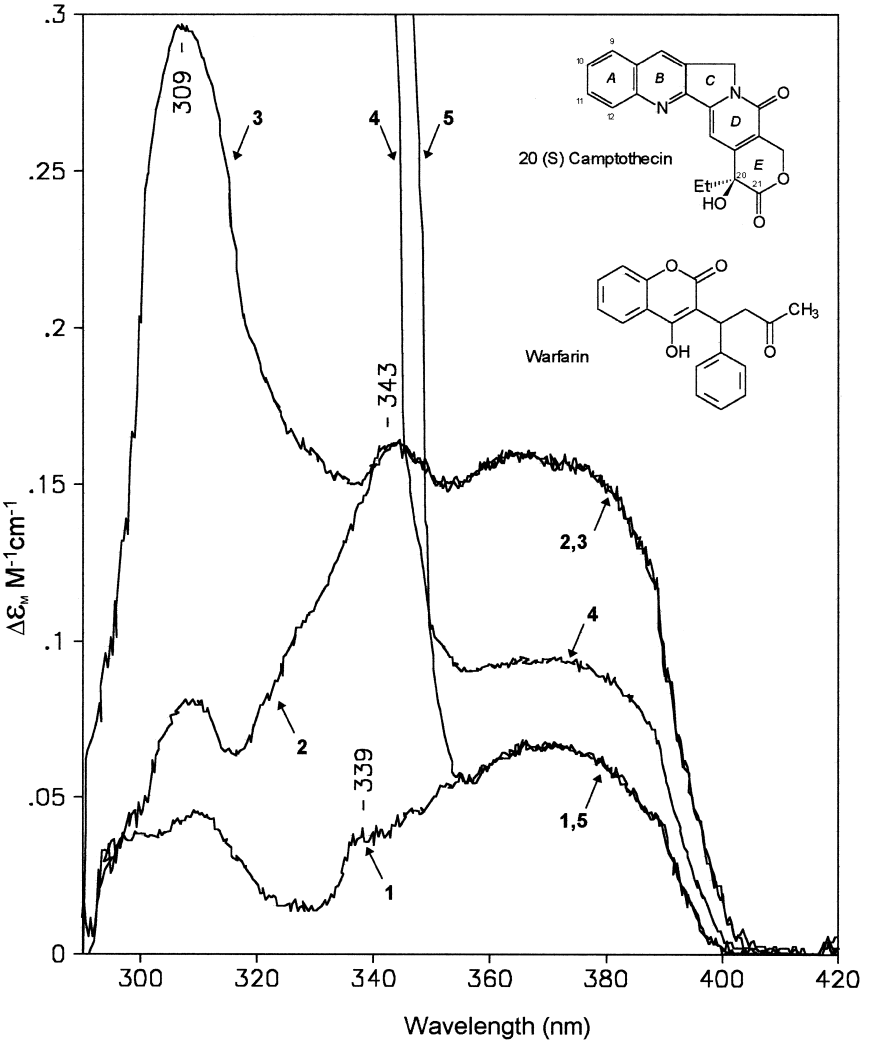

Fig. 2. 1,2: CD spectra of CPT's carboxylate form in PBS (1) and in complex with HSA (2). The concentrations of HSA (2×10^{-5} M) and CPT (2×10^{-5} M) in complex correspond to 1:1 molar ratio of components. 3–5: Titration of CPT/HSA complex by warfarin. Warfarin/CPT/HSA molar ratios were 5:1:1 (3); 250:1:1 (4), and 1000:1:1 (5). The spectra were recorded in a 1 cm cell.

Fig. 2 shows the results of titration of CPT/HSA complex by warfarin. CD signals of CPT and warfarin are well separated. Warfarin exhibits strong CD-band at ca. 309 nm, whereas free CPT shows only weak contribution in the 300–320 nm region, but well developed spectrum in the 330–400 nm region (Fig. 2, curve 1). As was shown before [10], interaction of CPT with HSA induces strong optical activity of CPT (Fig. 2, curve 2). Addition of warfarin to the CPT/HSA complex at 5:1:1 molar ratios of the components shows simple superposition of CD spectra of free warfarin and CPT/HSA complex (Fig. 2, curve 3). An increase in warfarin content up to the 250:1:1 ratio in warfarin/CPT/HSA reaction mixture (Fig. 2, curve 4) results in a pronounced decrease of a CD signal of the CPT/HSA complexes, and, finally, induced optical activity of CPT complexed with HSA totally disappears when the concentration of warfarin reaches 1000:1:1 molar ratio (Fig. 2, curve 5). At these conditions, CPT is totally replaced from its complex with HSA. The residual CD signal of CPT corresponds exactly to the optical activity of the free drug in the aqueous buffer solution (Fig. 2, compare curves 1 and 5 in the region 350–400 nm).

As was shown by Burke et al. [7] HSA binds CPT in a stoichiometry 1:1. From the analysis of the CD spectra of CPT/HSA complexes at different ratios of the components, the binding constant of CPTs carboxylate form with HSA was calculated to be ca. $1.1\pm0.5\times10^{7}$ M^{-1}. The following equation was used for calculation of the binding constant:

$$[W]\times\{[HSA]-\alpha[CPT]-\alpha/(K_{CPT}(1-\alpha))\}^{1} = 1+(1-\alpha)\,K_{CPT}\,(\alpha K_W)^{-1}$$

where [W], [HSA] and [CPT] are the concentrations of warfarin, HSA and CPT, respectively, K_{CPT} and K_W-binding constants for CPT and warfarin; α-degree of a HSA/CPT complex formation, determined as $\alpha=(I-I_F)/(I_B-I_F)$, where I is the intensity of the band 341 nm of CPT in a CD spectrum of reaction mixture, I_F is the intensity of the band 341 nm in a CD spectrum of free CPT, and I_B is the intensity of the band 341 nm for a reaction mixture with 100% CPT bound to HSA (measured at a 20 mg/ml concentration of HSA).

This calculated value of the CPT–HSA binding constant ($1.1\pm0.5\times10^{7}$ M^{-1}) is found to be in good agreement with the data published before ($1.2\pm0.1\times10^{6}$ M^{-1} [7], and 8.0×10^{6} M^{-1} [15]). The binding constant of warfarin to

HSA is known to be ca. 2.5×10^5 M^{-1} [15], i.e. ca. 50-fold weaker than that of CPT. So, it seems to be reasonable that total replacement of CPT by warfarin from CPT/HSA complexes was revealed when the concentration of warfarin was ca. 1000-fold higher than the concentration of CPT.

We have performed the similar CD measurements but for competitive binding of AZT and CPT with HSA. Titration by AZT does not induce any changes in CD spectra of CPT/HSA complexes up to the 1000:1:1 molar ratio of AZT, CPT and HSA. Hence, an absence of any changes in CD signals of CPT bound with HSA in the presence of ca. 1000-fold excess of AZT undoubtedly demonstrates that these two ligands occupy different binding sites of HSA.

Finally, the results of competitive binding of CPT and warfarin (a ligand which is bound in IIA subdomain of HSA) or CPT and AZT (a ligand which is bound in IIIA subdomain of HSA) to HSA show that the CPT-binding site is located within the IIA structural subdomain of the protein.

3.2. *HSA structural transformations induced by the CPT binding*

This question is addressed by CD and Raman spectroscopy analysis of CPT-induced changes in HSA conformation. Fig. 3 shows CD spectra of HSA and CPT/HSA complexes. The CD spectrum of HSA is typical for α-helical proteins [16]. The CD spectrum of the CPT/HSA complex was found to be practically identical (within the experimental error ca. 5%) to the spectrum of free HSA. So, the CD analysis shows that interaction with CPT does not induce significant (within ca. 30 peptide bonds) changes in the secondary structure of HSA.

This conclusion is confirmed by the Raman spectroscopic analysis of HSA and HSA/CPT complexes. Fig. 4a shows the Raman spectrum of HSA. The frequencies and intensities of Amide I (1654 cm^{-1}) and Amide III (ca. 1260–1300 cm^{-1}) bands of HSA are also typical for an essentially α-helical protein [17]. We used the methods described in [12] in order to analyse the Amide I band of HSA. The calculation revealed ca. 61% of α-helix, 16% of β-sheet and 23% of random coil. Hence, the secondary structure contents calculated from the Raman spectrum correspond very well to the data of X-ray diffraction [11]. Addition of CPT does not change the frequencies, intensities and shapes of Amide I and Amide III bands of HSA.

Does the binding of CPT induce local conformational changes of the protein? Raman spectra of proteins recorded under non-resonance conditions contain contributions from various amino acid side chain groups. Some of the side chain bands provide information of local side chain conformations or environments [18]. Fig. 4b compares the most informative parts of the Raman spectra of HSA (up) and CPT/HSA complexes (bottom), corresponding to the regions of S–S stretching vibrations (480–550 cm^{-1}), Fermi-resonance Tyr-doublet (800–860 cm^{-1}) and microenvironment-sensitive region of Trp vibrations (1340–1370 cm^{-1}).

The frequencies of S–S stretching vibrations of disulfide bridges of proteins change as a function of internal rotation about C–S and C–C bonds of the CC–SS–CC moiety. The vibrations in the region 500–510 cm^{-1} are assigned to a gauche–gauche–gauche (g–g–g) conformation, whereas a gauche–gauche–trans (g–g–t) rotamer gives the band at 515–525 cm^{-1}, and a trans–gauche–trans (t–g–t) at 535–545 cm^{-1}

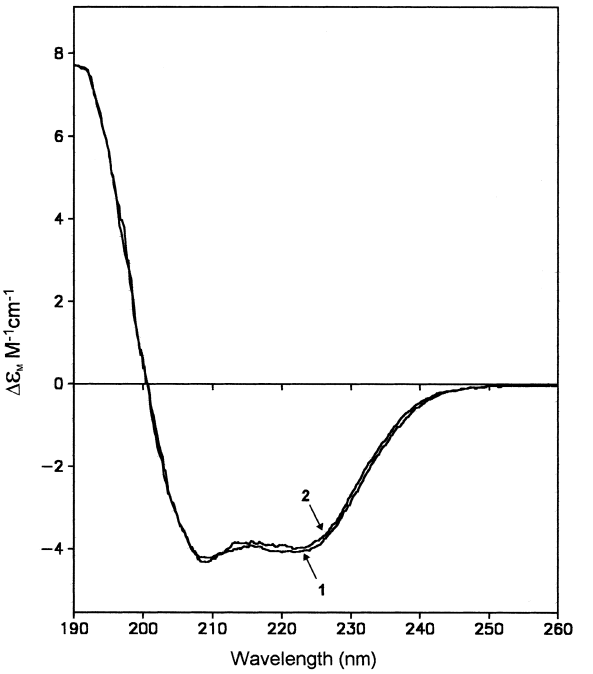

Fig. 3. CD spectra of HSA (1) and CPT/HSA complex (2) at the 1:1 drug/protein molar ratio. The spectra were measured in PBS, pH 7.4, at 25°C. Concentration of the components: 4×10^{-5} M. The spectrum was recorded in a 0.1 mm cell.

[18]. In the three-dimensional structure of HSA, 17 cysteines form disulfide linkages [11]. Calculations of the ratios of integrated intensities of the bands in the 480–550 cm^{-1} region corresponding to different rotamers in the Raman spectrum of HSA (Fig. 4b, top) show, that six disulfide bridges of HSA are in g–g–t, seven in g–g–g, and four other in t–g–t conformation. Addition of CPT leads to changes in relative integrated intensities of S–S bands in the Raman spectrum (Fig. 4b, bottom). Two disulfide bridges change their local conformation. Seven disulfide bonds are found to be in g–g–t, five in g–g–g, and five in t–g–t configurations. The data suggest CPT-induced transformation of two disulfide bridges of CPT from g–g–g to g–g–t and to t–g–t conformation.

The spectral region 800–860 cm^{-1} contains bands at about 830 and 850 cm^{-1} (so-called 'Fermi-resonance Tyr-doublet'), which are extremely sensitive to hydrogen bonding of the phenolic OH-groups [19]. The intensity ratio I_{850}/I_{830} reflects 'exposed' and/or 'buried' tyrosines. A ratio of about 2.5 indicates that the hydroxyl group is an acceptor of strong hydrogen bonding from a positive donor group [19]. This is the case of HSA (Fig. 4b, top): the ratio of bands within the observed Tyr-doublet shows that the main fraction of tyrosines of the protein is H-bonded with more positive donor groups. Addition of CPT (Fig. 4b, bottom) does not induce any modifications in the I_{850}/I_{830} ratio.

There is a unique Trp^{214} in the HSA molecule. The intensity of the 1360 cm^{-1} band is a marker of hydrophobicity of microenvironment of the indole ring. Its intensity grows as hydrophobicity of the environment increases [20]. The Raman spectrum shows that Trp^{214} of HSA is at least partially in hydrophobic environment but it becomes totally hydrophilic when going from free HSA to CPT/HSA complex (Fig. 4b).

Finally, the CD and Raman spectra show that the interaction of CPT with HSA does not modify (within the 5% ex-

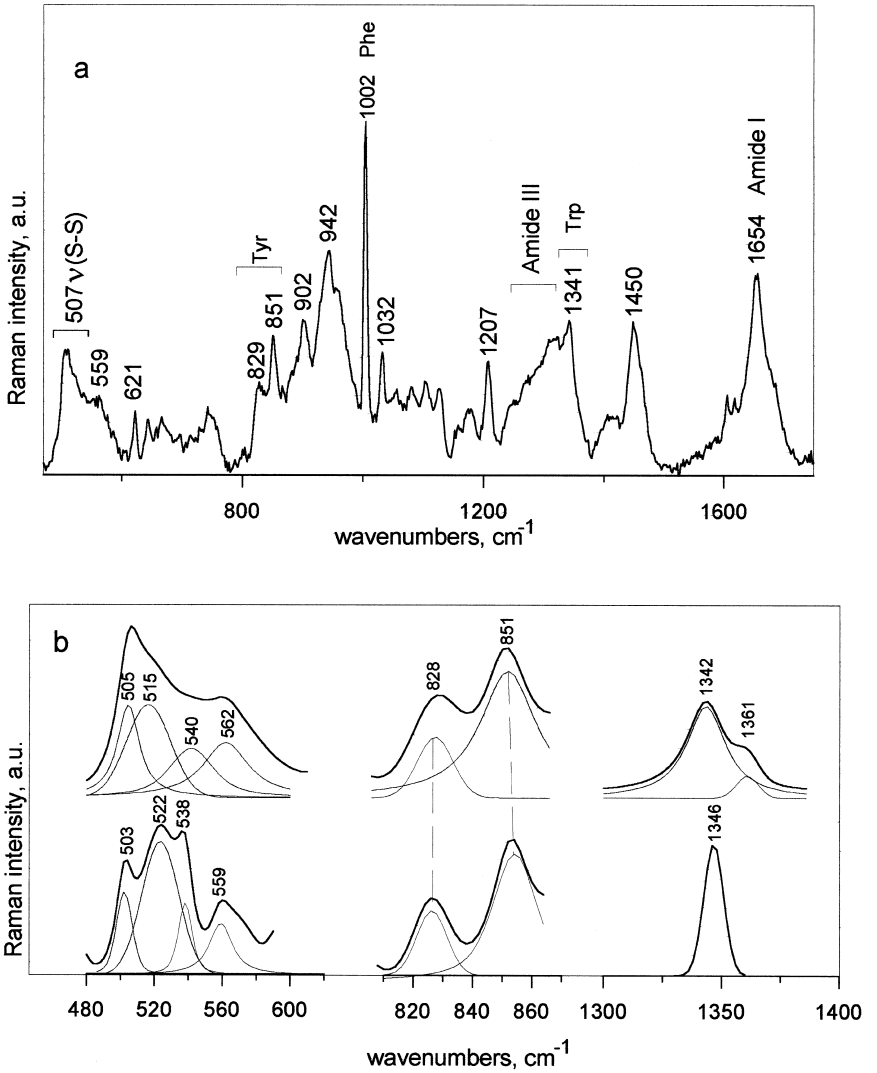

Fig. 4. A: Raman spectrum of HSA in PBS, pH 7.4. Laser power (514.5 nm): 300 mW. For other conditions see Section 2. B: The most informative regions of Raman spectra of HSA (top) and CPT/HSA complexes (bottom). The experimental spectra (thick lines) were decomposed on the components (thin lines) as described in [12]. For experimental conditions, see Section 2.

perimental error — ca. 30 peptide groups) the secondary structure of the protein, but changes configuration of at least two disulfide bridges. Interaction with CPT transfers a single Trp^{214} of HSA (located within the IIA subdomain) from the more hydrophobic to the hydrophilic environment.

HSA has a greater affinity for small, negatively charged hydrophobic molecules [15]. In this regard it is notable that HSA is the principal carrier of numerous pharmaceuticals in the blood which have otherwise limited solubility. If the drugs of CPT family, potent topo I inhibitors, are concerned, it is HSA that makes a significant impact on the drug stability [4–10] and may play a role of delivery machine in the blood. This paper shows that CPT binds within the IIA structural subdomain of HSA. It is known that both warfarin (occupying IIA) and triiodobenzoic acid (typical equipotent binder within IIA and IIIA subdomains of HSA) are located in that part of the cavity created by a smaller disulfide double loop (h5 and h6, Fig. 1), within the region of inter-domain connections [11]. So, it seems to be logical to suggest that the two disulfide bonds within the smaller disulfide double loop (connecting helices h4–h5 and h5–h6) change their conformation upon the binding of CPT. This transfer of the more compact g–g–g to the more extended g–g–t and t–g–t configurations should obviously lead to the relative movement of the protein structural domains. This relative rotation of domains may explain a transfer of the single Trp^{214}, located within the bottom half of h4 helice of the IIA structural subdomain (Fig. 1), from the more hydrophobic to the hydrophilic microenvironment.

Acknowledgements: This research was supported by Grant 1379 from the Association pour la Recherche Contre le Cancer (France) and, in part, by Grant HTECH.CRR961365 from the NATO, and Grant 96-04-48763 from the Russian Foundation for Basic Research. We thank Ms. Françoise Charton for technical assistance and Mr. E. Kryukov for critical reading of the manuscript and English correction.

References

[1] Gupta, M., Fujimori, A. and Pommier, Y. (1995) Biochim. Biophys. Acta 1262, 1–14.
[2] Capranico, G. and Zunino, F. (1995) Curr. Pharmac. Des. 1, 1–14.
[3] Hsiang, Y.-H. and Liu, L.F. (1988) Cancer Res. 48, 1722–1726.

[4] Burke, T.G., Mishra, A.K., Wani, M.C. and Wall, M.E. (1993) Biochemistry 32, 5352–5364.
[5] Burke, T.G. and Mi, Z. (1994) J. Med. Chem. 37, 40–46.
[6] Mi, Z. and Burke, T.G. (1994) Biochemistry 33, 10325–10336.
[7] Mi, Z. and Burke, T.G. (1994) Biochemistry 33, 12540–12545.
[8] F. Fleury, I. Kudelina, M. Manfait, A.J.P. Alix, and I.R. Nabiev, in: S.A. Asher, and P.B. Stein (Eds.), Raman Spectroscopy J. Wiley, Chichester, 1996, pp. 1128–1129.
[9] I. Nabiev, F. Fleury, I. Kudelina, Y. Pommier, F. Charton, J.-F. Riou, A.J.P. Alix, and M. Manfait, Biochem. Pharmacol., 1996, in press.
[10] Fleury, F., Kudelina, I. and Nabiev, I. (1997) FEBS Lett. 406, 151–156.
[11] X.M. He, and D.C. Carter, Nature 358 (1992) 209–215, and references herein.
[12] Berjot, M., Marx, J. and Alix, A.J.P. (1987) J. Raman Spectrosc. 18, 289–300.
[13] Kurono, Y., Ozeki, Y., Yamada, H., Takeuchi, T. and Ikeda, K. (1987) Chem. Pharmac. Bull. 35, 734–739.
[14] Ozeki, Y., Kurono, Y., Yotsuyangi, T. and Ikeda, K. (1980) Pharmac. Bull. 28, 535–540.
[15] U. Kragh-Hansen, Pharmac. Rev. 33 (1981) 17–53, and references herein.
[16] Manavalan, P. and Johnson Jr., W.C. (1983) Nature 305, 831–832.
[17] A.T. Tu, Raman Spectroscopy in Biology, J. Wiley, New York, 1982, and references herein.
[18] H. Fabian and P. Anzenbacher, Vibr. Spectrosc. 4 (1993) 125–148, and references herein.
[19] Siamwiza, M.N., Lord, R.C. and Chen, M.C. (1975) Biochemistry 14, 4870–4876.
[20] Miura, T., Takeuchi, H. and Harada, I. (1988) Biochemistry 27, 88–92.